

# Theoretical Spectroscopy of the $\text{N}_2\text{HAr}^+$ Complex

Vincent Brites,<sup>†</sup> Otto Dopfer,<sup>\*,‡</sup> and Majdi Hochlaf<sup>\*,§</sup>

Université Paris-Est Laboratoire Modélisation et Simulation Multi Echelle, MSME FRE 3160 CNRS, 5 boulevard Descartes, 77454 Marne-la-Vallée, France, Institut für Optik and Atomare Physik, Technische Universität Berlin, Hardenbergstrasse 36, D-10623, Berlin, Germany, and Université Paris-Est Laboratoire Modélisation et Simulation Multi Echelle, MSME FRE 3160 CNRS, 5 boulevard Descartes, 77454 Marne-la-Vallée, France

Received: July 22, 2008; Revised Manuscript Received: August 26, 2008

The six-dimensional potential energy surface of the electronic ground state of  $\text{N}_2\text{HAr}^+$  is determined by ab initio computations at the CCSD(T) level of theory. The potential energy surface is used to derive a set of spectroscopic data for  $\text{N}_2\text{HAr}^+$  and  $\text{N}_2\text{DAr}^+$  using second order perturbation theory. Full six-dimensional (6-D) rotation–vibration computations are also carried out using an analytical representation of the surface for  $J=0$  and 1, in order to deduce the rovibrational spectra of  $\text{N}_2\text{HAr}^+$  and its deuterated isotopomer. Our variationally determined anharmonic wavenumbers differ by less than  $15\text{ cm}^{-1}$  from the most accurate experimental values. Strong anharmonic resonances are found between the rovibrational levels of both cations even at low energies.

## I. Introduction

The proton-bound ionic complex  $\text{N}_2\text{HAr}^+$  was predicted to exist in 1995 by Kolbuszewski at the MP2 level of theory<sup>1</sup> with a relatively deep potential well toward dissociation into  $\text{N}_2\text{H}^+$  and Ar (dissociation energy  $D_e \approx 3000\text{ cm}^{-1}$ ). Two years later, the group at Basel<sup>2–4</sup> has characterized experimentally for the first time this cation by means of InfraRed PhotoDissociation (IRPD) spectroscopy and has accurately deduced its dissociation energy,  $D_0 = 2781.5 \pm 1.5\text{ cm}^{-1}$ , not far from the theoretical prediction. From the analysis of their IRPD spectra and the comparison to the available theoretical data,<sup>1</sup> these authors have tentatively determined the  $\nu_1$  fundamental (NH stretch) at  $\sim 2255\text{ cm}^{-1}$  and the  $\nu_s (= \nu_3)$  fundamental (HAr stretch) at  $\sim 2500\text{ cm}^{-1}$ . However, the IRPD spectral assignments proposed there were revised later, since this  $\nu_1$  value was completely out of the range of the CCSD(T) predictions of Botschwina and Oswald,<sup>5</sup>  $\nu_1 = 2519\text{ cm}^{-1}$ . Moreover, the previously derived value for  $\nu_1$  was also far from the direct absorption spectroscopy value of  $2505.5000\text{ cm}^{-1}$ , which is, however, the new commonly accepted evaluation of this stretching mode.<sup>6</sup> The  $\nu_2$  band origin (NN stretch) was also precisely determined at  $2041.1802\text{ cm}^{-1}$ .<sup>6</sup> Finally, several combination modes have been identified. Readers are referred to the recent review of Bieske and Dopfer<sup>7,8</sup> for more details.

In addition to the MP2 computations of Kolbuszewski<sup>1</sup> and the CCSD(T) three-dimensional (3-D) stretch-only vibrational Hamiltonian variational calculations of Botschwina and Oswald<sup>5,6</sup> discussed above, MP2/aug-cc-pVTZ calculations have been carried out for this cation by Dopfer et al.,<sup>4</sup> who have generated the 2-D intermolecular potential energy surface of the  $\text{N}_2\text{HAr}^+$  dimer and deduced a set of spectroscopic parameters, including equilibrium geometry and harmonic wavenumbers. Generally,

previous computations have noticed the existence of anharmonic resonances between the stretchings because of the mixed character of these modes that should be described as a combination of NH, NN and HAr elongation motions. Finally, an accurate experimental/theoretical equilibrium structure has been deduced by Verdes et al.<sup>9</sup> from the analysis of the rotationally resolved spectra obtained by IRPD and direct absorption and ab initio computations, yielding  $R_e(\text{NN}) = 1.0929\text{ \AA}$ ,  $R_e(\text{NH}) = 1.0752\text{ \AA}$ , and  $R_e(\text{HAr}) = 1.8854\text{ \AA}$ . These distances are in good accord with the most recent values deduced by Seki et al.<sup>10</sup> from their Fourier Transform microwave pure rotational spectra of six different isotopomers of  $\text{N}_2\text{HAr}^+$ .

For the deuteron-bound  $\text{N}_2\text{DAr}^+$  complex, similar investigations as for  $\text{N}_2\text{HAr}^+$  were performed. Briefly, these works have located the fundamentals at  $\nu_1$  (NN stretch) =  $2436.272\text{ cm}^{-1}$ ,<sup>11</sup> and  $\nu_2$  (ND stretch) =  $1593.6058\text{ cm}^{-1}$ .<sup>9</sup> A combination mode  $\nu_2 + 4\nu_s$ , which is found to strongly interact with  $\nu_1$ , occurs at  $2435.932\text{ cm}^{-1}$ .

Despite this significant amount of experimental and theoretical data on  $\text{N}_2\text{HAr}^+$  and  $\text{N}_2\text{DAr}^+$  in the literature, little is known about the bending modes, except their harmonic frequencies. The reliable pattern of the bending levels can, however, only be deduced from full 6-D variational calculations on a six-dimensional potential energy surface of the electronic ground state of this cationic species. Hence, accurate ab initio methods are used here in order to generate the 6-D potential energy surface (6-D PES) of the ground electronic state of  $\text{N}_2\text{HAr}^+$  covering its equilibrium geometry and the lowest dissociation pathway, leading to  $\text{N}_2\text{H}^+(\text{X}^1\Sigma^+)$  and  $\text{Ar}(^1\text{S})$ . Moreover, an analytical expression is deduced for this 6-D PES and used to derive a set of spectroscopic parameters for  $\text{N}_2\text{HAr}^+$  and its deuterated isotopomer using second order perturbation theory. This analytical expansion is also incorporated in full 6-D variational calculations using the method of Carter and Handy.<sup>12,13</sup> The rovibrational spectra of  $\text{N}_2\text{HAr}^+$  and  $\text{N}_2\text{DAr}^+$  are then deduced for  $J = 0$  and 1, allowing for reliable predictions for these two cations.

\* To whom correspondence should be addressed. E-mail: dopfer@physik.tu-berlin.de, hochlaf@univ-mlv.fr.

<sup>†</sup> Université Paris-Est Laboratoire Modélisation et Simulation Multi Echelle.

<sup>‡</sup> Institut für Optik and Atomare Physik, Technische Universität Berlin.

<sup>§</sup> Université Paris-Est Laboratoire Modélisation et Simulation Multi Echelle.

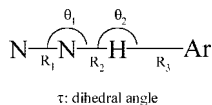


**Figure 1.** Definition of the internal coordinates of  $\text{N}_2\text{HAr}^+$ .

## II. Computational Methods

**a. Electronic Problem.** Sheng and Leszczynski<sup>14</sup> were emphasizing the importance of electron correlation in the treatment of  $\text{N}_2\text{HNg}^+$  molecular systems, where Ng is a rare gas. These authors came to the conclusion that DFT approaches are failing in treating these species and that only highly correlated methods, such as Coupled Cluster and Configuration Interaction methods, should be used for that purpose. Here, the 6-D PES of  $\text{N}_2\text{HAr}^+$  ( $X^1\Sigma^+$ ) was mapped using the coupled cluster method, CCSD(T), implemented in the MOLPRO program suite.<sup>15</sup> These calculations were carried out with two different basis sets. (1) In the larger basis set, the *spdfg* aug-cc-pV5Z basis set of Dunning was used for N and Ar, whereas the *spdf* aug-cc-pV5Z basis set was employed for H, resulting in 381 contracted Gaussian functions. (2) The smaller *spdf*(*f*) cc-pV5Z basis subset resulted in 222 contracted Gaussian functions.<sup>16,17</sup> These two basis sets were employed in order to compare the effect of the diffuse part of the basis sets on the electronic structure, the equilibrium geometry, and the rovibrational level pattern of  $\text{N}_2\text{HAr}^+$ . This effort is connected closely to the polarizability of Ar, which is better described with the larger basis set. Indeed, this quantity is computed to be  $\sim 10.08$  bohr<sup>3</sup> at the *spdfg* aug-cc-pV5Z/CCSD(T) level of theory, in close agreement with the experimental determination of 10.09 bohr<sup>3</sup>.<sup>18</sup> In contrast, similar calculations using the smaller basis set lead to  $\sim 8.8$  bohr<sup>3</sup>, a value that is 20% smaller than the experimental result. The counterpoise correction was also computed for the larger basis set in order to compare the influence of Basis Set Superposition Error (BSSE) on the spectroscopy of this cation. These three 6-D PESs were generated in the internal coordinates defined in Figure 1, comprising the three stretching coordinates  $R_1$  ( $R_{\text{NN}}$ ),  $R_2$  ( $R_{\text{NH}}$ ), and  $R_3$  ( $R_{\text{HAr}}$ ), the two in-plane bending angles  $\theta_1$  (NNH) and  $\theta_2$  (NHAr), and the torsional angle  $\tau$  between the NNH and NHAr planes. We calculated energies corresponding to different nuclear positions in the vicinity of the equilibrium geometry of  $\text{N}_2\text{HAr}^+(X^1\Sigma^+)$  and along the lowest energy fragmentation pathway, which leads to the lowest dissociation limit,  $\text{N}_2\text{H}^+(X^1\Sigma^+) + \text{Ar}(^1\text{S})$ . The geometries considered were in the ranges (in Å and degrees)  $0.9 \leq R_1 \leq 1.3$ ,  $0.85 \leq R_2 \leq 1.35$ ,  $1.6 \leq R_3 \leq 2.8$ ,  $50^\circ \leq \theta_{1,2} \leq 180^\circ$ , and  $0^\circ \leq \tau \leq 180^\circ$ , resulting in more than 300 geometries. For  $2 \leq R_3 \leq 2.8$ , a step of 0.1 Å is used for choosing the points. The constructed PES covers the energies up to  $\sim 15\,000$  cm<sup>-1</sup> above the minimum of  $\text{N}_2\text{HAr}^+(X^1\Sigma^+)$  and  $\sim 2700$  cm<sup>-1</sup> along the  $R_3$  coordinate. Subsequently, the calculated energies were fitted to the following polynomial expansion, where all points are equally weighted,

$$V(R_1, R_2, R_3, \theta_1, \theta_2, \tau) =$$

$$\sum_{ijklmn} c_{ijklmn} Q_1^i Q_2^j Q_3^k Q_4^l Q_5^m \cos(nQ_6) \quad (1)$$

with the three reduced stretching coordinates,  $Q_u = (R_u - R_u^{\text{ref}})/R_u$ , for  $u = 1-3$ , the two bending coordinates,  $Q_u = \theta_{u-3} - \theta_{u-3}^{\text{ref}}$ , for  $u = 4, 5$  ( $0^\circ \leq \theta_{u-3} \leq 180^\circ$ ), and the torsional angle,  $Q_6 = \tau - \tau^{\text{ref}}$  ( $0^\circ \leq \tau \leq 360^\circ$ ). The index “ref” refers to the reference geometry used during the fit (cf. Table 1). For the fit, the exponents in the expansion were restricted to  $i + j + k + l + m \leq 4$  and  $n \leq 2$ . For  $n \neq 0$ , only the terms, for which  $l$

**TABLE 1:** Equilibrium Distances ( $R_i$ , in Å), Rotational Constants ( $B_e$  and  $D_J$ , in cm<sup>-1</sup>), Harmonic Wavenumbers ( $\omega_e$ , in cm<sup>-1</sup>) and the Decomposition of the Normal Modes into the Internal Coordinates of  $\text{N}_2\text{HAr}^+(X^1\Sigma^+)$  and  $\text{N}_2\text{DAr}^+(X^1\Sigma^+)$

	$\text{N}_2\text{HAr}^+$	$\text{N}_2\text{DAr}^+$	
$R_1$	1.094 <sup>a</sup>		
	1.094 <sup>b</sup>		
	1.096 <sup>c</sup>		
	1.1081 <sup>d</sup>		
	1.1070 <sup>e</sup>		
	1.0949 <sup>f</sup>		
	1.098 <sup>g</sup>		
	1.071 <sup>a</sup>		
	1.074 <sup>b</sup>		
$R_2$	1.082 <sup>c</sup>		
	1.0831 <sup>d</sup>		
	1.0838 <sup>e</sup>		
	1.0755 <sup>f</sup>		
	1.074 <sup>g</sup>		
	1.920 <sup>a</sup>		
$R_3$	1.898 <sup>b</sup>		
	1.852 <sup>c</sup>		
	1.8346 <sup>d</sup>		
	1.8363 <sup>e</sup>		
	1.8871 <sup>f</sup>		
	1.909 <sup>g</sup>		
	0.0785 <sup>a</sup>	0.0784 <sup>a</sup>	
$B_e$	0.0793 <sup>b</sup>	0.0793 <sup>b</sup>	
	0.0810 <sup>c</sup>	0.0809 <sup>c</sup>	
	0.08136 <sup>d</sup>	0.07965 <sup>i</sup>	
	0.08126 <sup>e</sup>		
	0.07972 <sup>f</sup>		
$D_J$	$0.607 \times 10^{-7a}$	$0.611 \times 10^{-7a}$	
	$0.579 \times 10^{-7b}$	$0.583 \times 10^{-7b}$	
	$0.500 \times 10^{-7c}$	$0.503 \times 10^{-7c}$	
$\omega_1$ ( $\sigma^+$ )	2823 <sup>a</sup>	$0.82 R_1 - 0.57 R_2$	2542 <sup>a</sup>
	2784 <sup>b</sup>	$0.85 R_1 - 0.53 R_2$	2534 <sup>b</sup>
	2694 <sup>c</sup>	$0.88 R_1 - 0.46 R_2$	2494 <sup>c</sup>
	2659 <sup>d</sup>		2527 <sup>b</sup>
	2603 <sup>e</sup>		
$\omega_2$ ( $\sigma^+$ )	2783 <sup>f</sup>		
	2220 <sup>a</sup>	$0.97 R_1 + 0.25 R_2$	1778 <sup>a</sup>
	2204 <sup>b</sup>	$0.96 R_1 + 0.27 R_2$	1747 <sup>b</sup>
	2146 <sup>c</sup>	$0.94 R_1 + 0.31 R_2$	1674 <sup>c</sup>
	2049 <sup>d</sup>		1743 <sup>b</sup>
	2042 <sup>e</sup>		
$\omega_3$ ( $\sigma^+$ )	2195 <sup>f</sup>		
	173 <sup>a</sup>	$0.33 R_1 + 0.65 R_2 + 0.68 R_3$	171 <sup>a</sup>
	180 <sup>b</sup>	$0.33 R_1 + 0.65 R_2 + 0.68 R_3$	178 <sup>b</sup>
	200 <sup>c</sup>	$0.32 R_1 + 0.65 R_2 + 0.68 R_3$	197 <sup>c</sup>
	213 <sup>d</sup>		189 <sup>b</sup>
	210 <sup>e</sup>		
$\omega_4$ ( $\pi$ )	191 <sup>f</sup>		
	882 <sup>a</sup>	$-0.90 \theta_1 + 0.43 \theta_2$	667 <sup>a</sup>
	889 <sup>b</sup>	$-0.89 \theta_1 + 0.45 \theta_2$	671 <sup>b</sup>
	923 <sup>c</sup>	$-0.84 \theta_1 + 0.53 \theta_2$	693 <sup>c</sup>
	942 <sup>d</sup>		661 <sup>b</sup>
	919 <sup>e</sup>		
	876 <sup>f</sup>		
$\omega_5$ ( $\pi$ )	138 <sup>a</sup>	$0.80 \theta_1 + 0.60 \theta_2$	130 <sup>a</sup>
	143 <sup>b</sup>	$0.80 \theta_1 + 0.59 \theta_2$	134 <sup>b</sup>
	150 <sup>c</sup>	$0.81 \theta_1 + 0.58 \theta_2$	143 <sup>c</sup>
	172 <sup>d</sup>		148 <sup>b</sup>
	212 <sup>e</sup>		
156 <sup>f</sup>			

<sup>a</sup> This work: CCSD(T)/*spdfg* aug-cc-pV5Z including BSSE (381 cGTO) calculations. <sup>b</sup> This work: CCSD(T)/*spdfg* aug-cc-pV5Z (381 cGTO) calculations. <sup>c</sup> This work: CCSD(T)/*spdf* cc-pV5Z (222 cGTO) calculations. <sup>d</sup> MP2 (125 cGTO) calculations.<sup>1</sup> <sup>e</sup> MP2/full (203 cGTO) calculations.<sup>4</sup> <sup>f</sup> CCSD(T) (368 cGTO) calculations.<sup>6</sup> <sup>g</sup> Experimental value estimated from the analysis of the Fourier Transform microwave pure rotational spectra of six different isotopomers.<sup>10</sup> <sup>h</sup> CCSD(T) (368 cGTO) calculations.<sup>9</sup>

$\neq 0$ ,  $m \neq 0$  and  $l$ ,  $m$  and  $n$  have the same parity, were taken into account (see ref 19). Eventually, in total 71  $c_{ijklmn}$  coefficients were optimized using a least-squares procedure and the final values are listed in ref 20. The root-mean-square of the fit was less than 10 cm<sup>-1</sup>. Readers are referred to refs 21–27 for

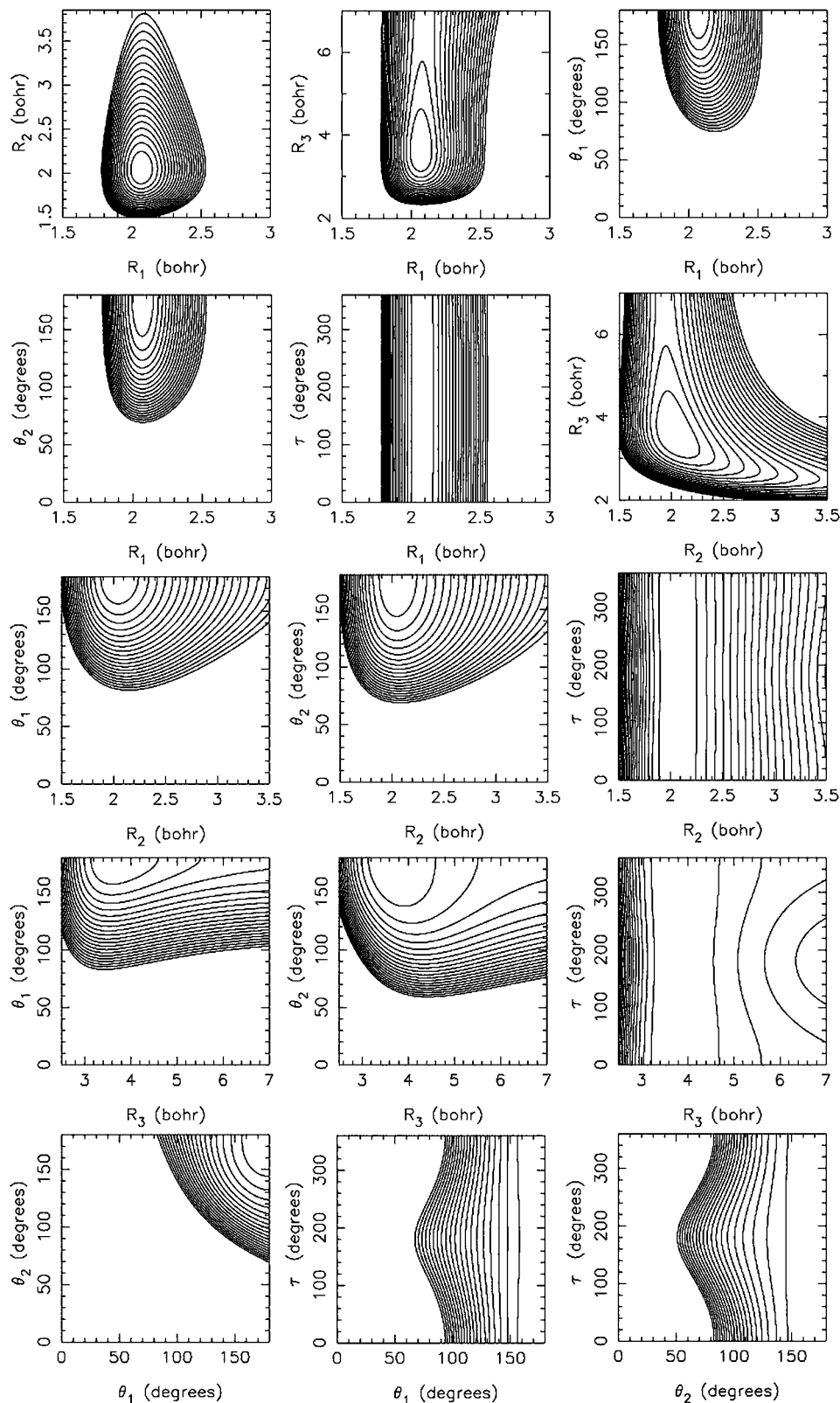


**Figure 2.** 2-D cuts through the 6-D PES of  $\text{N}_2\text{HAr}^+(\text{X}^1\Sigma^+)$ , obtained at the *spdf(g)* aug-cc-pV5Z/CCSD(T) level including the BSSE correction, for all 15 combinations of two of the internal coordinates. The other internal coordinates are kept fixed at their equilibrium values (cf. Table 1), except the contours involving  $\tau$ , which are given for  $\theta_1$  and/or  $\theta_2 = 150^\circ$ . The steps between the contours are  $1000 \text{ cm}^{-1}$ .

similar treatments of other linear tetratomic molecules, for which close agreement between calculations with accurate experimental data is achieved, further validating our theoretical approach.

**b. Nuclear Motion Problem.** The analytical representations of the 6-D PES were incorporated into perturbative and variational treatments of the nuclear problem. In the perturbative

approach, the 6-D PES was derived as a quartic force field in internal coordinates, which was subsequently transformed by L-tensor algebra into a quartic force field in dimensionless normal coordinates. This procedure enables the evaluation of the spectroscopic constants up to the fourth order, using the formula developed in refs 28 and 29. In the variational approach,

**TABLE 2: Variationally Calculated Rovibrational Levels of  $N_2HAr^+(X^1\Sigma^+)$  and Their Tentative Assignment<sup>a</sup>**

$J = 0$		$J = 1$			
$\sigma^+$		$\sigma^-$	$\pi$		
$(v_1, v_2, v_3, v_4^{14}, v_5^{15})$	energy	$(v_1, v_2, v_3, v_4^{14}, v_5^{15})$	energy		
(0,0,0,0 <sup>0</sup> ,0 <sup>0</sup> )	0	(0,0,0,1 <sup>1</sup> ,1 <sup>1</sup> )	1001	(0,0,0,0 <sup>0</sup> ,1 <sup>1</sup> )	162
(0,0,1,0 <sup>0</sup> ,0 <sup>0</sup> )	230	(0,0,1,1 <sup>1</sup> ,1 <sup>1</sup> )	1228	(0,0,1,0 <sup>0</sup> ,1 <sup>1</sup> )	394
(0,0,0,0 <sup>0</sup> ,2 <sup>0</sup> )	314	(0,0,0,1 <sup>1</sup> ,3 <sup>1</sup> )	1323	(0,0,0,0 <sup>0</sup> ,3 <sup>1</sup> )	568
(0,0,2,0 <sup>0</sup> ,0 <sup>0</sup> )	493	(0,0,2,1 <sup>1</sup> ,1 <sup>1</sup> )	1485	(0,0,2,0 <sup>0</sup> ,1 <sup>1</sup> )	660
(0,0,1,0 <sup>0</sup> ,2 <sup>0</sup> )	546	(0,0,1,1 <sup>1</sup> ,3 <sup>1</sup> )	1558	(0,0,1,0 <sup>0</sup> ,3 <sup>1</sup> )	803
(0,0,3,0 <sup>0</sup> ,0 <sup>0</sup> )	682	(0,0,3,1 <sup>1</sup> ,1 <sup>1</sup> )	1696	(0,0,0,1 <sup>1</sup> ,0 <sup>0</sup> )	828
(0,0,2,0 <sup>0</sup> ,2 <sup>0</sup> )	784	(0,0,2,1 <sup>1</sup> ,3 <sup>1</sup> )	1783	(0,0,3,0 <sup>0</sup> ,1 <sup>1</sup> )	973
(0,0,1,0 <sup>0</sup> ,4 <sup>0</sup> )	834	(0,0,1,1 <sup>1</sup> ,5 <sup>1</sup> )	1853	(0,0,1,1 <sup>1</sup> ,0 <sup>0</sup> )	1051
(0,0,4,0 <sup>0</sup> ,0 <sup>0</sup> )	929	(0,0,4,1 <sup>1</sup> ,1 <sup>1</sup> )	1947	(0,0,2,0 <sup>0</sup> ,3 <sup>1</sup> )	1065
(0,0,0,1 <sup>1</sup> ,1 <sup>1</sup> )	985	(0,0,0,2 <sup>0</sup> ,2 <sup>0</sup> )	1960	(0,0,4,0 <sup>0</sup> ,1 <sup>1</sup> )	1081
(0,0,2,0 <sup>0</sup> ,4 <sup>0</sup> )	1100	(0,0,3,1 <sup>1</sup> ,3 <sup>1</sup> )	2116	(0,0,0,1 <sup>1</sup> ,2 <sup>0</sup> )	1177
(0,0,5,0 <sup>0</sup> ,0 <sup>0</sup> )	1199	(0,0,5,1 <sup>1</sup> ,1 <sup>1</sup> )	2172	(0,0,3,0 <sup>0</sup> ,3 <sup>1</sup> )	1303
(0,0,1,1 <sup>1</sup> ,1 <sup>1</sup> )	1206	(0,0,1,2 <sup>0</sup> ,2 <sup>0</sup> )	2203	(0,0,0,0 <sup>0</sup> ,7 <sup>1</sup> )	1313
(0,0,4,0 <sup>0</sup> ,2 <sup>0</sup> )	1221	(0,0,4,1 <sup>1</sup> ,3 <sup>1</sup> )	2239	(0,0,2,1 <sup>1</sup> ,0 <sup>0</sup> )	1344
(0,0,0,1 <sup>1</sup> ,3 <sup>1</sup> )	1277	(0,0,0,2 <sup>0</sup> ,4 <sup>0</sup> )	2305	(0,0,5,0 <sup>0</sup> ,1 <sup>1</sup> )	1361
(0,0,3,0 <sup>0</sup> ,4 <sup>0</sup> )	1314	(0,0,3,1 <sup>1</sup> ,5 <sup>1</sup> )	2335	(0,0,1,1 <sup>1</sup> ,2 <sup>0</sup> )	1435
(0,0,2,1 <sup>1</sup> ,1 <sup>1</sup> )	1456	(0,0,2,2 <sup>0</sup> ,2 <sup>0</sup> )	2437	(0,0,0,1 <sup>1</sup> ,4 <sup>0</sup> )	1468
(0,0,5,0 <sup>0</sup> ,2 <sup>0</sup> )	1475	(0,0,5,1 <sup>1</sup> ,3 <sup>1</sup> )	2489	(0,0,4,0 <sup>0</sup> ,3 <sup>1</sup> )	1578
(0,0,1,1 <sup>1</sup> ,3 <sup>1</sup> )	1501	(0,0,1,2 <sup>0</sup> ,4 <sup>0</sup> )	2501	(0,0,3,1 <sup>1</sup> ,0 <sup>0</sup> )	1588
(0,0,0,1 <sup>1</sup> ,5 <sup>1</sup> )	1586			(0,0,3,0 <sup>0</sup> ,5 <sup>1</sup> )	1647
(0,0,7,0 <sup>0</sup> ,0 <sup>0</sup> )	1595			(0,0,2,1 <sup>1</sup> ,2 <sup>0</sup> )	1662
(0,0,0,2 <sup>0</sup> ,0 <sup>0</sup> )	1621			(0,0,5,0 <sup>0</sup> ,3 <sup>1</sup> )	1673
(0,0,6,0 <sup>0</sup> ,2 <sup>0</sup> )	1724			(0,0,1,1 <sup>1</sup> ,4 <sup>0</sup> )	1734
(0,0,2,1 <sup>1</sup> ,3 <sup>1</sup> )	1772			(0,0,4,0 <sup>0</sup> ,5 <sup>1</sup> )	1760
(0,0,1,1 <sup>1</sup> ,5 <sup>1</sup> )	1826			(0,0,2,0 <sup>0</sup> ,7 <sup>1</sup> )	1806
(0,0,1,2 <sup>0</sup> ,0 <sup>0</sup> )	1857			(0,0,4,1 <sup>1</sup> ,0 <sup>0</sup> )	1830
(0,0,4,0 <sup>0</sup> ,6 <sup>0</sup> )	1893			(0,0,0,2 <sup>0</sup> ,1 <sup>1</sup> )	1868
(0,0,3,0 <sup>0</sup> ,8 <sup>0</sup> )	1909			(0,0,7,0 <sup>0</sup> ,1 <sup>1</sup> )	1880
(0,0,8,0 <sup>0</sup> ,0 <sup>0</sup> )	1938			(0,0,3,1 <sup>1</sup> ,2 <sup>0</sup> )	1912
(0,0,4,1 <sup>1</sup> ,1 <sup>1</sup> )	1962			(0,0,6,0 <sup>0</sup> ,3 <sup>1</sup> )	1961
(0,0,3,1 <sup>1</sup> ,3 <sup>1</sup> )	1970			(0,0,2,1 <sup>1</sup> ,4 <sup>0</sup> )	1968
(0,1,0,0 <sup>0</sup> ,0 <sup>0</sup> )	2056			(0,0,1,2 <sup>0</sup> ,1 <sup>1</sup> )	2033
(0,0,2,1 <sup>1</sup> ,5 <sup>1</sup> )	2064			(0,0,1,1 <sup>1</sup> ,6 <sup>0</sup> )	2082
(0,0,2,2 <sup>0</sup> ,0 <sup>0</sup> )	2078			(0,0,4,0 <sup>0</sup> ,7 <sup>1</sup> )	2118
(0,0,5,0 <sup>0</sup> ,6 <sup>0</sup> )	2131			(0,0,8,0 <sup>0</sup> ,1 <sup>1</sup> )	2146
(0,0,4,0 <sup>0</sup> ,8 <sup>0</sup> )	2149			(0,0,3,1 <sup>1</sup> ,3 <sup>1</sup> )	2175
(0,0,9,0 <sup>0</sup> ,0 <sup>0</sup> )	2186			(0,0,4,1 <sup>1</sup> ,2 <sup>0</sup> )	2183
(0,0,5,1 <sup>1</sup> ,1 <sup>1</sup> )	2201			(0,0,7,0 <sup>0</sup> ,3 <sup>1</sup> )	2221
(0,0,4,1 <sup>1</sup> ,3 <sup>1</sup> )	2220			(0,0,3,1 <sup>1</sup> ,4 <sup>0</sup> )	2224
(0,0,8,0 <sup>0</sup> ,2 <sup>0</sup> )	2255			(0,0,0,2 <sup>0</sup> ,3 <sup>1</sup> )	2236
(0,1,1,0 <sup>0</sup> ,0 <sup>0</sup> )	2284			(0,1,0,0 <sup>0</sup> ,1 <sup>1</sup> )	2244
(0,0,3,1 <sup>1</sup> ,5 <sup>1</sup> )	2332			(0,0,6,0 <sup>0</sup> ,5 <sup>1</sup> )	2265
(0,0,3,2 <sup>0</sup> ,0 <sup>0</sup> )	2367			(0,0,2,1 <sup>1</sup> ,5 <sup>1</sup> )	2285
(0,1,0,0 <sup>0</sup> ,2 <sup>0</sup> )	2376			(0,0,2,2 <sup>0</sup> ,1 <sup>1</sup> )	2305
(0,0,6,0 <sup>0</sup> ,6 <sup>0</sup> )	2409			(0,0,5,1 <sup>1</sup> ,0 <sup>0</sup> )	2348
(0,0,5,0 <sup>0</sup> ,8 <sup>0</sup> )	2412			...	...
(0,0,10,0 <sup>0</sup> ,0 <sup>0</sup> )	2418			(0,1,0,1 <sup>1</sup> ,0 <sup>0</sup> )	2937
(0,0,6,1 <sup>1</sup> ,1 <sup>1</sup> )	2437				
(0,0,5,1 <sup>1</sup> ,3 <sup>1</sup> )	2476				
(0,0,9,0 <sup>0</sup> ,2 <sup>0</sup> )	2496				
(1,0,0,0 <sup>0</sup> ,0 <sup>0</sup> )	2518				
...	...				
(0,2,3,0 <sup>0</sup> ,0 <sup>0</sup> )	2719				
(1,0,1,0 <sup>0</sup> ,0 <sup>0</sup> )	2740				
(1,0,0,0 <sup>0</sup> ,2 <sup>0</sup> )	2848				
(1,0,2,0 <sup>0</sup> ,0 <sup>0</sup> )	3025				
(1,0,3,0 <sup>0</sup> ,0 <sup>0</sup> )	3272				

<sup>a</sup> These data are derived from the 6-D PES obtained at the *spdf(g)* aug-cc-pV5Z/CCSD(T) level including the BSSE correction. See text for more details. All values are in cm<sup>-1</sup>.

the method of Carter and Handy was employed,<sup>12,13</sup> which takes all couplings between all angular momenta into account, leading to relatively large Hamiltonian matrices for tetratomic species. To reduce the size of these matrices, the following contraction scheme was employed. First, 2-D contractions were done for  $R_1$  and  $R_3$ , and the resulting functions were then combined with

the stretching functions associated with  $R_2$ . The 3-D stretching functions were contracted and stocked for later use. Four different contractions were performed for the bending coordinates, two by combining the  $\theta_1$  and  $\theta_2$  basis functions with  $\cos(0\tau)$  and  $\cos(1\tau)$  and two with  $\sin(1\tau)$  and  $\sin(2\tau)$ . The resulting functions were then contracted to the primitive  $\tau$

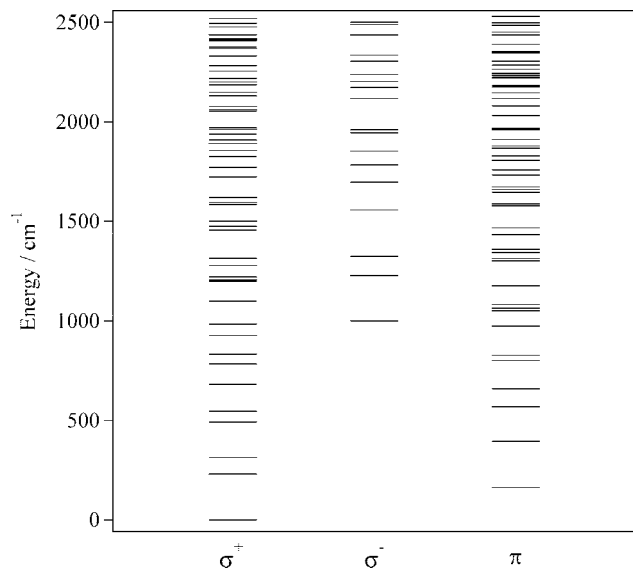


**Figure 3.** Pattern of the variationally calculated rovibrational levels of N<sub>2</sub>HAr<sup>+</sup>(X<sup>1</sup>Σ<sup>+</sup>) for  $J = 0$  and  $J = 1$  (cf. Table 2).

functions,  $\cos(0\tau)$  to  $\cos(M\tau)$  and  $\sin(1\tau)$  to  $\sin(M\tau)$ . The rovibrational levels were then obtained after diagonalization of the Hamiltonian matrix written in the basis formed by the 3-D contracted stretching functions and the contracted bending functions (for  $J = 0$ ) and the eigenfunctions of the rigid rotor (for  $J \neq 0$ ). Consequently, the resulting Hamiltonian matrix is formed only by 1-D or 2-D integrals, reducing the cost for the variational calculations.<sup>12,13</sup> Details of the basis set used for these calculations are given in refs 22, 27, 30, and 31. The accuracy of these calculations is  $\sim 1$  cm<sup>-1</sup> for the converged levels. The accuracy of the computed rovibrational energies is better than 20 cm<sup>-1</sup> for the converged levels. The rotational constants are believed to be accurate to within 0.01 cm<sup>-1</sup>.

### III. Results and Discussion

**a. Characteristics of the Six-Dimensional Potential Energy Surface (6-D PES) of N<sub>2</sub>HAr<sup>+</sup>(X<sup>1</sup>Σ<sup>+</sup>).** Figure 2 depicts the 2-D cuts through the 6-D PES of N<sub>2</sub>HAr<sup>+</sup>(X<sup>1</sup>Σ<sup>+</sup>), obtained at the *spdffg* aug-cc-pV5Z/CCSD(T) level and including the BSSE correction, along two of the internal coordinates, with the remaining internal coordinates kept fixed at their equilibrium values (cf. Table 1), except for those involving the torsion  $\tau$ , which are given for  $\theta_1$  and/or  $\theta_2 = 150^\circ$ . In each cut, 20 contours are plotted in steps of 1000 cm<sup>-1</sup>. The 2-D cuts were also generated through the 6-D PES without the BSSE correction and through the 6-D PES computed with the smaller basis set. Comparison between these 2-D cuts reveals that these three PESs present similar shapes so that the following discussion is valid for three of them. Inspection of Figure 2 reveals that, with the exception of the NN ( $R_1$ ) stretching, this PES is very flat along all internal coordinates, in particular, the cuts involving  $R_2$  (NH) and  $R_3$  (HAr). Hence, low anharmonic wavenumbers are expected for some of the normal modes. The cuts along the  $R_3$  distance display a shallow minimum, corresponding to the equilibrium geometry of N<sub>2</sub>HAr<sup>+</sup>(X<sup>1</sup>Σ<sup>+</sup>), with a slow rise in energy for large  $R_3$  distances up to the lowest intermolecular dissociation limit. By bending both in-plane angles, local minima can be found along the torsion coordinate for  $\tau \approx 90^\circ$  and  $270^\circ$ . These minima are located higher in energy than the global linear minimum of N<sub>2</sub>HAr<sup>+</sup>(X<sup>1</sup>Σ<sup>+</sup>) and correspond to transient species formed during the isomerization of linear N<sub>2</sub>HAr<sup>+</sup> toward less

**TABLE 3: Variationally Calculated Anharmonic Wavenumbers ( $\nu_i$ , in cm<sup>-1</sup>) of N<sub>2</sub>HAr<sup>+</sup>(X<sup>1</sup>Σ<sup>+</sup>) and N<sub>2</sub>DAr<sup>+</sup>(X<sup>1</sup>Σ<sup>+</sup>) and Comparison to Experimental Values**

$\nu_1$ ( $\sigma^+$ )	2517.9 <sup>a</sup>	2438.8 <sup>a</sup>
	2522.1 <sup>b</sup>	2438.7 <sup>b</sup>
	2478.2 <sup>c</sup>	2423.3 <sup>c</sup>
	2519.0 <sup>d</sup>	2441 <sup>e</sup>
	2505.5000 <sup>e</sup>	2436.272 <sup>h</sup>
$\nu_2$ ( $\sigma^+$ )	2056.4 <sup>a</sup>	1611.6 <sup>a</sup>
	2062.8 <sup>b</sup>	1597.8 <sup>b</sup>
	2055.5 <sup>c</sup>	1617.8 <sup>c</sup>
	1987.0 <sup>d</sup>	1559 <sup>e</sup>
	2041.1802 <sup>e</sup>	1593.6058 <sup>h</sup>
$\nu_3$ ( $\sigma^+$ )	230.0 <sup>a</sup>	197.7 <sup>a</sup>
	236.0 <sup>b</sup>	202.7 <sup>b</sup>
	256.4 <sup>c</sup>	230.8 <sup>c</sup>
	205.0 <sup>d</sup>	195 <sup>e</sup>
	199.2 <sup>f</sup>	
$\nu_4$ ( $\pi$ )	828.3 <sup>a</sup>	633.0 <sup>a</sup>
	841.9 <sup>b</sup>	640.8 <sup>b</sup>
	910.0 <sup>c</sup>	680.2 <sup>c</sup>
$\nu_5$ ( $\pi$ )	162.0 <sup>a</sup>	142.3 <sup>a</sup>
	163.5 <sup>b</sup>	144.5 <sup>b</sup>
	168.9 <sup>c</sup>	157.7 <sup>c</sup>
$\nu_1 + \nu_3$	2739.9 <sup>a</sup>	
	2748.2 <sup>b</sup>	
	2777.0 <sup>c</sup>	
	2756.0 <sup>d</sup>	
	2755.62 <sup>i</sup>	
$\nu_2 + 3\nu_3$	2718.5 <sup>a</sup>	
	2715.6 <sup>b</sup>	
	2658.0 <sup>b</sup>	
$\nu_2 + 4\nu_3$	2707.34 <sup>i</sup>	
		2420.2 <sup>a</sup>
		2422.8 <sup>b</sup>
		2408.4 (2442.6) <sup>j</sup>
		2435.932 <sup>k</sup>

<sup>a</sup> This work: CCSD(T)/*spdffg* aug-cc-pV5Z including BSSE (381 cGTO) calculations. <sup>b</sup> This work: CCSD(T)/*spdffg* aug-cc-pV5Z (381 cGTO) calculations. <sup>c</sup> This work: CCSD(T)/*spdffg* cc-pV5Z (222 cGTO) calculations. <sup>d</sup> CCSD(T) (368 cGTO) calculations. <sup>e</sup> Experimental value. <sup>f</sup> Experimental value estimated from the analysis of the Fourier Transform microwave pure rotational spectra of six different isotopomers. <sup>g</sup> CCSD(T) (368 cGTO) calculations. <sup>h</sup> Experimental data. <sup>i</sup> Experimental value. <sup>j</sup> CCSD(T) calculations. <sup>k</sup> Experimental data.<sup>11</sup>

stable isomers of the same sum formula. Similar behavior has already been noticed in the 6-D PESs of some linear tetratomic molecules, such as NCCN,<sup>21</sup> C<sub>3</sub>O,<sup>24</sup> CCNN,<sup>25</sup> and C<sub>3</sub>S.<sup>26</sup>

Close examination of the cuts in Figure 2 shows couplings between several internal coordinates. For example, the NN ( $R_1$ ) and NH ( $R_2$ ) elongations are slightly coupled together. Much stronger couplings are identified between the NH ( $R_2$ ) and the HAr ( $R_3$ ) bonds. The two bendings are also coupled together and with the HAr stretch coordinate. These couplings are confirmed by the decomposition of the normal modes into the internal coordinates (cf. Table 1 for more details). In particular, the  $\nu_3$  mode is a strong mixture of the NN, HN, and HAr displacements. The resulting anharmonic resonances complicate the assignments of vibrational quantum numbers to the rovibrational levels observed in both the experimental and theoretical spectra (vide infra). The bendings are coupled with the HN and HAr stretches. Finally, the torsion is coupled with all the other internal coordinates.

Table 1 compares the linear equilibrium geometry of N<sub>2</sub>HAr<sup>+</sup>(X<sup>1</sup>Σ<sup>+</sup>) deduced from the present analysis with previous theoretical and experimental determinations. Our parameters,  $R_1 = 1.094$  (1.094) Å,  $R_2 = 1.074$  (1.071) Å, and  $R_3 = 1.898$

**TABLE 4: Variationally Calculated Rovibrational Levels of  $N_2\text{D}\text{Ar}^+(X^1\Sigma^+)$  and their Tentative Assignment<sup>a</sup>**

$J = 0$				$J = 1$	
$\sigma^+$		$\sigma^-$		$\pi$	
$(\nu_1, \nu_2, \nu_3, \nu_4^{14}, \nu_5^{15})$	energy	$(\nu_1, \nu_2, \nu_3, \nu_4^{14}, \nu_5^{15})$	energy	$(\nu_1, \nu_2, \nu_3, \nu_4^{14}, \nu_5^{15})$	energy
(0,0,0,0 <sup>0</sup> ,0 <sup>0</sup> )	0	(0,0,0,1 <sup>1</sup> ,1 <sup>1</sup> )	788	(0,0,0,0 <sup>0</sup> ,1 <sup>1</sup> )	142
(0,0,1,0 <sup>0</sup> ,0 <sup>0</sup> )	198	(0,0,1,1 <sup>1</sup> ,1 <sup>1</sup> )	982	(0,0,1,0 <sup>0</sup> ,1 <sup>1</sup> )	339
(0,0,0,0 <sup>0</sup> ,2 <sup>0</sup> )	288	(0,0,0,1 <sup>1</sup> ,3 <sup>1</sup> )	1081	(0,0,0,0 <sup>0</sup> ,3 <sup>1</sup> )	471
(0,0,2,0 <sup>0</sup> ,0 <sup>0</sup> )	401	(0,0,2,1 <sup>1</sup> ,1 <sup>1</sup> )	1182	(0,0,2,0 <sup>0</sup> ,1 <sup>1</sup> )	541
(0,0,1,0 <sup>0</sup> ,2 <sup>0</sup> )	481	(0,0,1,1 <sup>1</sup> ,3 <sup>1</sup> )	1272	(0,0,0,1 <sup>1</sup> ,0 <sup>0</sup> )	633
(0,0,0,0 <sup>0</sup> ,4 <sup>0</sup> )	597	(0,0,0,1 <sup>1</sup> ,5 <sup>1</sup> )	1393	(0,0,1,0 <sup>0</sup> ,3 <sup>1</sup> )	666
(0,0,3,0 <sup>0</sup> ,0 <sup>0</sup> )	620	(0,0,3,1 <sup>1</sup> ,1 <sup>1</sup> )	1402	(0,0,3,0 <sup>0</sup> ,1 <sup>1</sup> )	761
(0,0,2,0 <sup>0</sup> ,2 <sup>0</sup> )	682	(0,0,2,1 <sup>1</sup> ,3 <sup>1</sup> )	1478	(0,0,1,1 <sup>1</sup> ,0 <sup>0</sup> )	833
(0,0,0,1 <sup>1</sup> ,1 <sup>1</sup> )	775	(0,0,0,2 <sup>0</sup> ,2 <sup>0</sup> )	1544	(0,0,2,0 <sup>0</sup> ,3 <sup>1</sup> )	840
(0,0,1,0 <sup>0</sup> ,4 <sup>0</sup> )	796	(0,0,1,1 <sup>1</sup> ,5 <sup>1</sup> )	1595	(0,0,0,1 <sup>1</sup> ,2 <sup>0</sup> )	873
(0,0,3,0 <sup>0</sup> ,2 <sup>0</sup> )	869	(0,0,3,1 <sup>1</sup> ,3 <sup>1</sup> )	1655	(0,0,1,0 <sup>0</sup> ,5 <sup>1</sup> )	928
(0,0,0,0 <sup>0</sup> ,6 <sup>0</sup> )	922	(0,0,0,1 <sup>1</sup> ,7 <sup>1</sup> )	1732	(0,0,4,0 <sup>0</sup> ,1 <sup>1</sup> )	1003
(0,0,2,0 <sup>0</sup> ,4 <sup>0</sup> )	970	(0,0,2,1 <sup>1</sup> ,5 <sup>1</sup> )	1742	(0,0,2,1 <sup>1</sup> ,0 <sup>0</sup> )	1023
(0,0,1,1 <sup>1</sup> ,1 <sup>1</sup> )	973	(0,0,1,2 <sup>0</sup> ,2 <sup>0</sup> )	1759	(0,0,3,0 <sup>0</sup> ,3 <sup>1</sup> )	1041
(0,0,5,0 <sup>0</sup> ,0 <sup>0</sup> )	1008			(0,0,0,0 <sup>0</sup> ,7 <sup>1</sup> )	1045
(0,0,0,1 <sup>1</sup> ,3 <sup>1</sup> )	1063			(0,0,1,1 <sup>1</sup> ,2 <sup>0</sup> )	1110
(0,0,1,0 <sup>0</sup> ,6 <sup>0</sup> )	1141			(0,0,2,0 <sup>0</sup> ,5 <sup>1</sup> )	1136
(0,0,3,0 <sup>0</sup> ,4 <sup>0</sup> )	1177			(0,0,0,1 <sup>1</sup> ,4 <sup>0</sup> )	1215
(0,0,2,1 <sup>1</sup> ,1 <sup>1</sup> )	1189			(0,0,3,1 <sup>1</sup> ,0 <sup>0</sup> )	1255
(0,0,0,2 <sup>0</sup> ,0 <sup>0</sup> )	1233			(0,0,4,0 <sup>0</sup> ,3 <sup>1</sup> )	1270
(0,0,6,0 <sup>0</sup> ,0 <sup>0</sup> )	1250			(0,0,1,0 <sup>0</sup> ,7 <sup>1</sup> )	1276
(0,0,1,1 <sup>1</sup> ,3 <sup>1</sup> )	1269			(0,0,2,1 <sup>1</sup> ,2 <sup>0</sup> )	1296
(0,0,5,0 <sup>0</sup> ,2 <sup>0</sup> )	1319			(0,0,3,0 <sup>0</sup> ,5 <sup>1</sup> )	1338
(0,0,3,1 <sup>1</sup> ,1 <sup>1</sup> )	1397			(0,0,0,0 <sup>0</sup> ,9 <sup>1</sup> )	1356
(0,0,1,0 <sup>0</sup> ,8 <sup>0</sup> )	1406			(0,0,0,2 <sup>0</sup> ,1 <sup>1</sup> )	1370
(0,0,1,2 <sup>0</sup> ,0 <sup>0</sup> )	1421			(0,0,6,0 <sup>0</sup> ,1 <sup>1</sup> )	1412
(0,0,7,0 <sup>0</sup> ,0 <sup>0</sup> )	1440			(0,0,4,1 <sup>1</sup> ,0 <sup>0</sup> )	1430
(0,0,3,0 <sup>0</sup> ,6 <sup>0</sup> )	1458			(0,0,5,0 <sup>0</sup> ,3 <sup>1</sup> )	1442
(0,0,2,1 <sup>1</sup> ,3 <sup>1</sup> )	1487			(0,0,2,0 <sup>0</sup> ,7 <sup>1</sup> )	1464
(0,0,0,2 <sup>2</sup> ,2 <sup>2</sup> )	1499			(0,0,3,1 <sup>1</sup> ,2 <sup>0</sup> )	1488
(0,0,0,2 <sup>0</sup> ,2 <sup>0</sup> )	1510			(0,0,4,0 <sup>0</sup> ,5 <sup>1</sup> )	1520
(0,0,6,0 <sup>0</sup> ,2 <sup>0</sup> )	1551			(0,0,1,2 <sup>0</sup> ,1 <sup>1</sup> )	1534
(0,1,0,0 <sup>0</sup> ,0 <sup>0</sup> )	1611			(0,0,1,0 <sup>0</sup> ,9 <sup>1</sup> )	1546
(0,0,4,1 <sup>1</sup> ,1 <sup>1</sup> )	1618			(0,0,2,1 <sup>1</sup> ,4 <sup>0</sup> )	1589
(0,0,2,2 <sup>0</sup> ,0 <sup>0</sup> )	1636			(0,0,7,0 <sup>0</sup> ,1 <sup>1</sup> )	1611
(0,0,8,0 <sup>0</sup> ,0 <sup>0</sup> )	1659			(0,0,5,1 <sup>1</sup> ,0 <sup>0</sup> )	1630
(0,0,4,0 <sup>0</sup> ,6 <sup>0</sup> )	1676			(0,0,6,0 <sup>0</sup> ,3 <sup>1</sup> )	1657
(0,0,3,1 <sup>1</sup> ,3 <sup>1</sup> )	1698			(0,0,4,1 <sup>1</sup> ,2 <sup>0</sup> )	1678
(0,0,1,2 <sup>2</sup> ,2 <sup>2</sup> )	1720			(0,0,5,0 <sup>0</sup> ,5 <sup>1</sup> )	1701
(0,0,1,2 <sup>0</sup> ,2 <sup>0</sup> )	1729				
...					
(0,1,2,0 <sup>0</sup> ,0 <sup>0</sup> )	2030				
(1,0,0,0 <sup>0</sup> ,0 <sup>0</sup> )	2439				
(0,1,4,0 <sup>0</sup> ,0 <sup>0</sup> )	2420				

<sup>a</sup> These data are derived from the 6-D PES obtained at the *spdf(g)* aug-cc-pV5Z/CCSD(T) level including the BSSE correction. See text for more details. All values are in  $\text{cm}^{-1}$ .

(1.920) Å obtained at the *spdf(g)* aug-cc-pV5Z/CCSD(T) level of theory without and with (in parentheses) BSSE correction agree quite well with the previous MP2 (125 cGTO), MP2 (203 cGTO) and the CCSD(T) results of Kolbuszewski,<sup>1</sup> Dopfer et al.,<sup>4</sup> and Botschwina et al.,<sup>6</sup> respectively (Table 1). When compared to the equilibrium structure deduced from the microwave spectra of Seki et al.,<sup>10</sup> our values for  $R_1$  and  $R_2$  differ by less than 0.004 Å from theirs. For  $R_3$ , the difference between our (with and without the BSSE correction) and their value reaches 0.011 Å, probably due to the flatness of the PES along this coordinate, which is better described in our 6-D treatment as compared to previous theoretical efforts. Using the smaller basis set (i.e., *spdf*) cc-pV5Z without BSSE correction), a surprisingly good agreement with previous works is also noticeable, despite the fact that this basis set not fully describes the polarizability of Ar, which is the main relevant quantity for the formation of this complex (via charge-induced dipole interaction).

When compared to their corresponding diatomic and triatomic fragments, the  $R_1$  separation (NN stretch) in  $N_2\text{H}\text{Ar}^+$  of 1.098 Å (see Table 1) is slightly longer than the NN distance in the neutral  $N_2(X^1\Sigma_g^+)$  diatomic (1.09768 Å<sup>32</sup>) but remains distinctly shorter than in  $N_2^+(X^2\Sigma_g^+)$  (1.11642 Å<sup>32</sup>). The weakening of the NN bond in the  $N_2\text{H}\text{Ar}^+$  complex is most likely a signature of a charge transfer occurring during the formation of the bonds between  $N_2$ , H, and Ar in this complex. Then, the HAr distance ( $R_3 = 1.852$  Å) of this complex is strongly shortened compared to the neutral HAr diatomic ( $R_e = 3.6$  Å for  $\text{H}\text{Ar}(\text{X})$ <sup>33</sup>) but still longer than the equilibrium distance (of 1.28 Å<sup>32</sup>) in  $\text{H}\text{Ar}^+$ . Again, this is consistent with the partial electron transfer from  $N_2$  to  $\text{H}\text{Ar}^+$ . Finally, the NN and NH distances in  $N_2\text{H}\text{Ar}^+$  are slightly longer than those of  $N_2\text{H}^+$ , probably because of small electron transfer to the weak HAr bond. Similar effects have already been observed for other charge-transfer complexes. Interested readers are referred to refs 22, 23 for further examples.

The dissociation energy ( $D_0$ ) of the  $\text{N}_2\text{HAr}^+$  complex was measured precisely as  $2781.5 \pm 1.5 \text{ cm}^{-1}$ .<sup>2</sup> This value is in good agreement with the  $D_e$  value of  $\sim 2820$  (2720)  $\text{cm}^{-1}$  deduced from our 6-D PES, obtained at the *spdf(g)* aug-cc-pV5Z/CCSD(T) without (with) BSSE correction. The accuracy of the calculated value is expected to be  $\sim 100 \text{ cm}^{-1}$ , according to previous calculations and due to our experience in calculating this quantity.<sup>22,23</sup> When compared to previous theoretical data, our dissociation energy is in close accord with both the MP2 (203 cGTO) and the CCSD(T) (368 cGTO) determinations of Dopfer et al. ( $D_e = 2881 \text{ cm}^{-1}$ )<sup>4</sup> and of Botschwina et al.<sup>6</sup> ( $D_e = 2819 \text{ cm}^{-1}$ ), respectively. The less precise MP2 calculations of Kolbuszewski<sup>1</sup> lead, however, to a quite high value ( $D_e = 3088 \text{ cm}^{-1}$ ), which is out of the range of our and the other previous determinations.

**b. Spectroscopic Properties and Rovibrational Spectrum of  $\text{N}_2\text{HAr}^+(\text{X}^1\Sigma^+)$ .** The  $\text{N}_2\text{HAr}^+(\text{X}^1\Sigma^+)$  cation has five vibrational modes, namely three stretching modes,  $\nu_{1-3}$  ( $\sigma^+$ ), and two doubly degenerate bending modes,  $\nu_{4-5}$  ( $\pi$ ). If the bending modes are excited, then there are two vibrational angular momenta  $l_4$  and  $l_5$ , for which only the projection of  $l = l_4 + l_5$  has to be considered. The variable  $l$  varies from  $|l_4 - l_5|$  to  $l_4 + l_5$  in steps of two. The rotational angular momentum  $J$  needs to be greater or equal to  $l$  ( $J = l, l + 1, l + 2, \dots$ ). Table 1 lists the rotational constants ( $B_e$  and  $D_j$ ) and the harmonic wavenumbers ( $\omega_i$ ) for  $\text{N}_2\text{HAr}^+(\text{X}^1\Sigma^+)$ . This table gives also a comparison between our computed data and the corresponding previously determined quantities. Concerning the harmonic wavenumbers, our values computed at the *spdf(g)* aug-cc-pV5Z/CCSD(T) level of theory with and without BSSE correction, compare relatively well with previous CCSD(T) calculations. The differences are less than  $25 \text{ cm}^{-1}$  with previous works.

Let us now concentrate on the comparison of our three 6D-PESs computed at the *spd(f)* cc-pV5Z/CCSD(T) level and the *spdf(g)* aug-cc-pV5Z/CCSD(T) level with and without BSSE correction. As expected, Table 1 shows that the inclusion of diffuse functions is crucial for a better description of the bonding, the electronic structure, and therefore, the spectroscopy of this complex. For instance, the values for  $\omega_1$ ,  $\omega_2$ , and  $\omega_4$  derived at the *spd(f)* cc-pV5Z/CCSD(T) level of theory are quite different from the others, whereas  $\omega_3$  and  $\omega_5$  show relatively better accord with previous calculations. More generally, such discrepancies between the data obtained using a smaller or larger basis set are expected for these molecular systems due to the flatness of the PESs along the corresponding coordinates and of the importance of electron correlation in the description of their bonding. For instance, electron correlation effects should change drastically the shape of the PESs, especially near the equilibrium minimum, leading to different second order derivatives and consequently to quite different  $\omega$  values. For these molecular systems, only full-dimensional variationally computed spectra on 6-D PESs can lead to reliable spectroscopic information, which can directly be compared to the experimental data (see below).

Table 2 lists the variationally calculated rovibrational spectrum of the 6-D PES of  $\text{N}_2\text{HAr}^+(\text{X}^1\Sigma^+)$  for  $J = 0$  and  $J = 1$  obtained at the *spdf(g)* aug-cc-pV5Z/CCSD(T) level including the BSSE correction. Figure 3 displays the pattern of these levels up to  $2500 \text{ cm}^{-1}$  above the zero point energy. The accuracy of the variationally determined wavenumbers is expected to be  $\sim 20 \text{ cm}^{-1}$ , comparably to similar works on other tetratomic systems.<sup>21-27</sup> Table 2 and Figure 3 clearly show the high density of rovibrational levels even for energies as low as  $1500 \text{ cm}^{-1}$  above the zero point vibrational energy, favoring their mutual

interactions and resulting anharmonic resonances. The anharmonic resonances are mixing the initial rovibrational wave functions, making their equivocal assignment a quite difficult task. In our assignment, we were also guided by the perturbatively computed spectrum using the 6-D PESs. Table 2 lists the tentatively assigned spectrum for all rovibrational levels up to  $2500 \text{ cm}^{-1}$  above the zero point vibrational energy and for the pure  $(1,0,\nu_3,0^0,0^0)$  and  $(0,\nu_2,0,0^0,0^0)$  stretching series up to  $3200 \text{ cm}^{-1}$  above the zero point vibrational energy.

As can be seen in Table 3, our fundamentals computed at the *spdf(g)* aug-cc-pV5Z/CCSD(T) level (without BSSE correction) are  $\nu_1$  (NH stretch) = 2522.1,  $\nu_2$  (NN stretch) = 2062.8,  $\nu_3$  (HAr stretch) = 236.0,  $\nu_4$  (trans bending) = 841.9 and  $\nu_5$  (cis bending) = 163.5 (all values are in  $\text{cm}^{-1}$ ), respectively. These values change to  $\nu_1 = 2517.9$ ,  $\nu_2 = 2056.4$ ,  $\nu_3 = 230.0$ ,  $\nu_4 = 828.3$  and  $\nu_5 = 162.0$  when including the BSSE correction. The above-mentioned differences between data derived from the 6-D PES for the harmonic wavenumbers with and without BSSE are clearly reduced when considering the 6-D variationally computed anharmonic wavenumbers. Our results represent reliable predictions for the bending modes. When compared to the  $\text{N}_2\text{H}^+$  monomer, the NH and NN stretches show substantial redshifts of 712 and 195  $\text{cm}^{-1}$ , respectively. These are indicative of the perturbation of the corresponding bonds arising from the formation of this complex.

In the following, we will be discussing only the data derived from our 6D-PES computed at the *spdf(g)* aug-cc-pV5Z/CCSD(T) level and including the BSSE correction. For the  $\nu_1$  and  $\nu_2$  modes, our values agree quite well with the most precise experimental determinations of these quantities, with differences of less than  $16 \text{ cm}^{-1}$  (Table 3). Such differences are within the expected accuracy of our computations. In order to further rationalize this observation, we have also generated the 3-D PES of the ground-state of  $\text{N}_2\text{H}^+(\text{X}^1\Sigma^+)$  at the Coupled Cluster level of theory using the same basis set (*spdf(g)* aug-cc-pV5Z). The details of these calculations and of the corresponding theoretical data will be published separately.<sup>34</sup> Briefly, these computations show that the NH stretch ( $\nu_1$ ) of  $\text{N}_2\text{H}^+(\text{X}^1\Sigma^+)$  is calculated at  $3234 \text{ cm}^{-1}$ , matching with the experimental value of Keim et al.<sup>35</sup> The  $\text{N}_2\text{H}^+(\text{X}^1\Sigma^+)$   $\nu_2$  mode (NN stretch) is calculated to be  $2265 \text{ cm}^{-1}$ , which is  $7 \text{ cm}^{-1}$  higher than the experimental value of Foster and McKellar.<sup>36</sup>

The HAr stretch wavenumber ( $\nu_3$ ) in  $\text{N}_2\text{HAr}^+$  is calculated to be  $230.0 \text{ cm}^{-1}$ , which may be compared to the experimental estimate of  $199 \text{ cm}^{-1}$  derived from the analysis of the rotational spectrum.<sup>10</sup> Interestingly, Table 2 shows that the  $(0,0,\nu_3,0,0)$  vibrational series presents an inverted anharmonicity character. Indeed, one can clearly see that its corresponding harmonic  $\omega$  value ( $\omega_3 = 173 \text{ cm}^{-1}$ ) value is lower than its anharmonic  $\nu$  value ( $\nu_3 = 230 \text{ cm}^{-1}$ ). This is closely related to the flatness of the PES along the corresponding normal coordinate. Similarly, the  $(0,0,0,0,\nu_5)$  vibrational series exhibits such an inverted anharmonicity behavior. Here again,  $\omega_5 (=138 \text{ cm}^{-1})$  is lower than  $\nu_5 (=162 \text{ cm}^{-1})$ , which is also a signature of the flatness of the PES along this bending coordinate. These features are commonly occurring for the low frequency modes in charge-transfer molecular systems, such as  $\text{N}_2\text{CO}^+$  and  $\text{N}_4^+$ .<sup>23,24</sup> Generally, the harmonic approximation is not appropriate to generate accurate rovibrational spectra for this type of molecular species.

Dealing with combination modes, the  $\nu_1 + \nu_3$  band has been identified at  $2755.62 \text{ cm}^{-1}$  by Nizkorodov et al.<sup>2</sup> This value is differing by  $\sim 16 \text{ cm}^{-1}$  from our computed value of  $2740 \text{ cm}^{-1}$  (cf. Table 2). This deviation is still within the expected accuracy

of our computations. Hence, the couplings between the vibrational modes, at least between the  $\nu_1$  and  $\nu_3$  stretch, are well described by our 6-D PES. Similarly, our computed wavenumber for  $\nu_2 + 3\nu_3$  ( $= 2718.5 \text{ cm}^{-1}$ , cf. Table 2) shows a good agreement with the experimental value of  $2707.34 \text{ cm}^{-1}$ , signature here again of the good description of the couplings between the  $\nu_2$  and  $\nu_3$  modes.

**c. Spectroscopic Properties and Rovibrational Spectrum of  $\text{N}_2\text{D}\text{Ar}^+(\text{X}^1\Sigma^+)$ .** In Tables 1 and 4 are listed a set of spectroscopic parameters and the variationally calculated spectrum for  $\text{N}_2\text{D}\text{Ar}^+(\text{X}^1\Sigma^+)$ , respectively. The isotopic shifts (in  $\text{cm}^{-1}$ ) are computed variationally to be  $\Delta\nu_1 = 79$ ,  $\Delta\nu_2 = 445$ ,  $\Delta\nu_3 = 32$ ,  $\Delta\nu_4 = 195$  and  $\Delta\nu_5 = 20$ . Hence, the five vibrational modes are significantly affected by substituting the H atom by D, since the H atom is located in the middle of this tetratomic molecule and because of the mixing of all five modes together (cf. the decomposition of the normal modes into the internal coordinates given in Table 1). Concerning the accuracy of the  $\omega$  and the  $\nu$  values given in these tables, we refer to the discussion carried out above for  $\text{N}_2\text{H}\text{Ar}^+$ . Shortly, using the parameters evaluated for the 6-D PES obtained at the *spdf(g)* aug-cc-pV5Z/CCSD(T) level with BSSE correction, our  $\nu_1$  and  $\nu_2$  wavenumbers are computed to be  $2438.8$  and  $1611.6 \text{ cm}^{-1}$ , respectively, which are displaced by less than  $\sim 20 \text{ cm}^{-1}$  from the most accurate experimental determinations of Verdes et al.<sup>9</sup> and Verbraak et al.<sup>11</sup> However, our  $\nu_3$  anharmonic wavenumber computed at  $197.7 \text{ cm}^{-1}$  is very close to the value deduced from the CCSD(T) computations of Verdes et al.<sup>9</sup> (see Table 3). As for the normal isotopomer, a high density of rovibrational states is noticed, which allows anharmonic resonances to occur. This has been confirmed recently, for instance, by the IR spectrum of  $\text{N}_2\text{D}\text{Ar}^+$  in the energy domain  $2400\text{--}2500 \text{ cm}^{-1}$ , where a strong Fermi interaction between the  $\nu_1$  and  $\nu_2 + 4\nu_3$  bands is reported by Verbraak et al.<sup>11</sup> More generally, the features pointed out for  $\text{N}_2\text{H}\text{Ar}^+$  and detailed in the previous sections are also valid for the deuterated species.

#### IV. Conclusions

Large-scale ab initio computations are performed in order to generate the 6-D PES of the electronic ground-state of the  $\text{N}_2\text{H}\text{Ar}^+$  cationic species using the Coupled Cluster methods and different basis sets and corrections. The analytical forms of these 6-D PESs are incorporated later into perturbative and full 6-D variational treatments of the nuclear motions, in order to derive a set of spectroscopic data for the  $\text{N}_2\text{H}\text{Ar}^+$  and  $\text{N}_2\text{D}\text{Ar}^+$  isotopomers and their rovibrational spectra up to  $3200 \text{ cm}^{-1}$ . Our data, obtained at the largest level of theory, are in good agreement with the most accurate experimental measurements. Surprisingly, our computations show a very minor effect of the BSSE correction on the spectroscopy of this charge transfer complex. The simulation of the IR spectrum of these species requires the generation of the 6-D dipole moment surface of  $\text{N}_2\text{H}\text{Ar}^+$  and our PES and a variational treatment, which will be done in the near future.

**Acknowledgment.** Part of this study was supported by the Deutsche Forschungsgemeinschaft (DO 729/2) and the Fonds der Chemischen Industrie.

**Supporting Information Available:** Table of polynomial expansion coefficients. This material is available free of charge via the Internet at <http://pubs.acs.org>.

#### References and Notes

- (1) Kolbuszewski, M. *Chem. Phys. Lett.* **1995**, *244*, 39.
- (2) Nizkorodov, S. A.; Spinelli, Y.; Bieske, E. J.; Maier, J. P.; Dopfer, O. *Chem. Phys. Lett.* **1997**, *265*, 303.
- (3) Nizkorodov, S. A., PhD thesis, University of Basel (1997).
- (4) Dopfer, O.; Olkhov, R. V.; Maier, J. P. *J. Phys. Chem. A* **1999**, *103*, 2982.
- (5) Botschwina, P.; Oswald, R. Conference on Electron Correlation in Spectroscopy and Dynamics, Kaiserslautern, 1998 (unpublished), Poster P38.
- (6) Botschwina, P.; Oswald, R.; Linnartz, H.; Verdes, D. *J. Phys. Chem.* **2000**, *113*, 2736.
- (7) Bieske, E. J.; Dopfer, O. *Chem. Rev.* **2000**, *100*, 3963, and references therein.
- (8) Dopfer, O. *Faraday Discuss.* **2001**, *118*, 171.
- (9) Verdes, D.; Linnartz, H.; Botschwina, P. *Chem. Phys. Lett.* **2000**, *329*, 228, and references therein.
- (10) Seki, K.; Sumiyoshi, Y.; Endo, Y. *J. Chem. Phys.* **2002**, *117*, 9750.
- (11) Verbraak, H.; Snels, M.; Botschwina, P.; Linnartz, H. *J. Chem. Phys.* **2006**, *124*, 224315.
- (12) Bramley, M. J.; Carter, S.; Handy, N. C.; Mills, I. M. *J. Mol. Spectro.* **1993**, *157*, 301.
- (13) Carter, S.; Pinnavaia, N.; Handy, N. C. *Chem. Phys. Lett.* **1995**, *240*, 400.
- (14) Sheng, Y.; Leszczynski, J. *J. Phys. Chem. A* **2002**, *106*, 12095.
- (15) MOLPRO is a package of ab initio programs written by H. J. Werner and P.J. Knowles. Further details are available at <http://www.molpro.net>.
- (16) Dunning, T. H. *J. Chem. Phys.* **1989**, *90*, 1007.
- (17) Woon, D. E.; Dunning, T. H., Jr. *J. Chem. Phys.* **1993**, *98*, 1358.
- (18) Kraka, E.; Cremer, D.; Spoerel, U.; Merke, I.; Stahl, W.; Dreizler, H. *J. Chem. Phys.* **1995**, *99*, 12466, and references therein.
- (19) Strey, G.; Mills, I. M. *J. Mol. Spectro.* **1976**, *59*, 103.
- (20) Can be found in the Supporting Information Available section.
- (21) Hochlaf, M. *J. Mol. Spectro.* **2001**, *207*, 269.
- (22) Hochlaf, M.; Léonard, C.; Ferguson, E. E.; Rosmus, P.; Reinsch, E. A.; Carter, S.; Handy, N. C. *J. Chem. Phys.* **1999**, *111*, 4948.
- (23) Léonard, C.; Rosmus, P.; Carter, S.; Handy, N. C. *J. Phys. Chem. A* **1999**, *103*, 1846.
- (24) Hochlaf, M. *J. Mol. Spectro.* **2001**, *210*, 284.
- (25) Hochlaf, M. *J. Chem. Phys.* **2000**, *113*, 5763.
- (26) Zaidi, A.; Lahmar, S.; Ben Lakhdar, Z.; Rosmus, P.; Hochlaf, M. *Theor. Chem. Acta* **2005**, *114*, 341.
- (27) Hochlaf, M. *Trends Chem. Phys.* **2005**, *12*, 1.
- (28) Papousek, D.; Aliev, M. R. *Molecular Vibrational-Rotational Spectra*; Elsevier Scientific Publishing: New York, 1982.
- (29) Mills, I. M. In *Molecular Spectroscopy: Modern Research*; Rao, K. N., Mathews, C. W., Eds; Academic Press: New York, 1972.
- (30) Richter, F.; Hochlaf, M.; Rosmus, P.; Gatti, F.; Meyer, H.-D. *J. Chem. Phys.* **2004**, *120*, 1306.
- (31) Lakin, N.; Hochlaf, M.; Chambaud, G.; Rosmus, P. *J. Chem. Phys.* **2001**, *115*, 3664.
- (32) <http://webbook.nist.gov>.
- (33) Partridge, H.; Bauschlicher, C. W. *Mol. Phys.* **1999**, *96*, 705.
- (34) In preparation.
- (35) Keim, E. R.; Owrutsky, J. C.; Coe, J. V.; Saykally, R. J. *J. Chem. Phys.* **1990**, *93*, 3111.
- (36) Foster, S. C.; McKellar, A. R. W. *J. Chem. Phys.* **1984**, *81*, 3424.